Pergamon

Int. J. Heat Mass Transfer. Vol. 40, No. 4, pp. 857–867, 1997

0017–9310/97 $17.00+0.00

PII: S0017-9310(96)00115-9

Oscillatory instability analysis of Bénard–Marangoni convection in a rotating fluid with internal heat generation

MING-I CHAR and KO-TA CHIANG

Department of Applied Mathematics, National Chung Hsing University, Taichung, Taiwan 402, Republic of China

and

JONG-JHY JOU

Department of Applied Mathematics, Feng Chia University, Taichung, Taiwan 407, Republic of China

(*Received* 11 *October* 1995 *and in final form* 23 *April* 1996)

Abstract—The onset of oscillatory instability of Bénard–Marangoni convection in a horizontal fluid layer, subject to the Coriolis force and internal heat generation, is investigated. The upper surface is deformably free and the lower surface is rigid. The characteristic equations of the perturbed state are solved numerically, using the Runge–Kutta–Gill's shooting method and the Broyden's method. The Crispation number C is significant for the occurrence of oscillatory modes. The results show that smaller absolute values of critical Marangoni number $|M_c|$ and frequency σ_{ic} take place at larger values of Crispation number C. The effect of the rotation is stabilizing, while that of the internal heat generation is strongly destabilizing. The Biot number B_i and the Bond number B_o increase the critical condition. For oscillatory modes, the Prandtl number Pr would decrease the stability. Copyright © 1996 Elsevier Science Ltd.

INTRODUCTION

The Bénard–Marangoni convective instability of a horizontal fluid layer, through the mutual interaction of the thermal buoyancy and surface tension, was initially investigated by Nield [1]. The Rayleigh–Bénard convective instability has been intensively studied by Chandrasekhar [2], Drazin and Reid [3], Sparrow *et al.* [4] and Ferm and Wollkind [5]. The Marangoni convective instability, due to the variation of surface tension with temperature, has been theoretically analyzed by Pearson [6] and Vidal and Acrivos [7]. Usually, a free upper surface can be deformed under the normal and shear stresses, unless its surface tension is of an infinite degree. Therefore, the surface defection, when considering the Bénard–Marangoni convective instability, was taken into account by Scriven and Sternling [8], Smith [9] and Davis and Homsy [10].

When the Crispation effect of a deformably free upper surface is considered, the system may set in oscillatorily. Benguira and Depassier [11, 12] investigated the oscillatory instabilities in the Rayleigh–Bénard and Bénard–Marangoni problems with a deformable free surface. Pérez-García and Carneiro [13] made a systematic study on the linear stability of the Bénard–Marangoni convective instability and focused on the effect of a free-surface deformation. Wilson [14, 15] studied the effect of a uniform magnetic field on the onset of convective instability in a horizontal thin liquid layer. Both stationary Bénard–Marangoni convection [14] and oscillatory Marangoni convection [15] were treated.

The non-linear temperature distribution in a horizontal layer can be created by an internal heat generation. The onset of thermal instability in a horizontal fluid layer, subject to an internal heat generation, has been analyzed by Sparrow *et al.* [4] and Roberts [16]. Gasser and Kazimi [17] and Kaviany [18] studied the effect of the internal heat generation on the onset of convection in a porous medium.

The Coriolis force in a rotating system has a significant influence on the onset of convective instability. Chandrasekhar [2] and Veronis [19] investigated such a Rayleigh–Bénard type with a linear temperature profile. Friedrich and Rudraiah [20] examined the Marangoni type in the presence of a non-uniform temperature gradient. Pearlstein [21] extended such a problem to a doubly diffusive fluid layer. Recently, Goldstein *et al.* [22] have carried out a detailed study of the linear stability of the onset of convection in a uniformly rotating right circular cylinder heated from below. They found that, whenever the azimuthal wavenumber of the mode is non-

NOMENCLATURE

a	wavenumber of the small disturbance
Bi	Biot number, HL/K
Bo	Bond number, $\rho g L^2/\gamma$
C	Crispation number, $\mu\kappa/\gamma L$
D_{ij}	rate of the strain tensor in the fluid
$\mathbf{e}_z$	unit vector in the z-direction
g	gravitational acceleration
H	heat transfer coefficient
$\mathcal{J}$	Taylor number, $4\Omega^2 L^4/\nu^2$
K	thermal conductivity
L	thickness of the fluid layer
M	Marangoni number, $\tau\Delta T L/\mu\kappa$
$\mathbf{n}$	normal unit vector at the free upper surface
N_S	dimensionless heat source strength, $QL^2/\kappa\Delta T$
p	pressure
Pr	Prandtl number, ν/κ
Q	uniformly distributed volumetric internal heat generation in the fluid layer
R	Rayleigh number, $\alpha g \Delta T L^3/\nu\kappa$
t	time
$\mathbf{t}$	tangential unit vectors at the free upper surface
T	temperature
V	velocity (u, v, w)
W	amplitude of the disturbance of velocity
x, y, z	coordinates
Z	amplitude of the disturbance of the non-dimensional surface deflection.

Greek symbols

α	thermal expansion coefficient of the fluid density
γ	surface tension
ΔT	difference of temperature across the fluid layer
ζ	vorticity of the fluid layer, $\mathbf{e}_z \cdot \nabla \times V'$
η	position of the upper free surface
Θ	amplitude of the disturbance of temperature
κ	thermal diffusivity
μ	viscosity of fluid
ν	kinematic viscosity of fluid
ρ	density of fluid
σ_r, σ_i	real and imaginary growth rates with time
τ	surface tension gradient with respect to temperature, $\partial\gamma/\partial T$
Ω	uniform angular velocity.

Superscripts

$\bar{}$	steady-state quantity
$'$	perturbed quantity.

Subscripts

c	critical state
o	referential quantity.

zero, the instability is a Hopf bifurcation, which results in precessing spiral patterns.

In this study, we consider the onset of oscillatory modes of Bénard–Marangoni convective instability in a fluid layer, subject to the Coriolis force and an internal heat generation. The stability analysis is based on the linear stability theory. The effects of the Prandtl number, the Taylor number, the internal heat generation, the surface tension of a deformable upper free surface and its thermal conductivity on the onset of oscillatory Bénard–Marangoni instability are considered.

MATHEMATICAL FORMULATION

A horizontal fluid layer of thickness L is subjected to a rotation about a vertical axis with a constant angular velocity Ω, as shown in Fig. 1. The upper surface is deformably free and conductive. The surface tension γ adopts the linear form [4–13]:

$$\gamma = \gamma_0 - \tau(T - T_0), \tag{1}$$

where γ_0 is a reference value, τ is the rate of change with temperature and the reference temperature T_0. The lower surface is rigid and isothermal.

The Boussinesq's approximation is assumed [1–3]:

$$\rho = \rho_0[1 - \alpha(T - T_0)], \tag{2}$$

where α is the coefficient of thermal expansion and ρ_0 is the reference density.

The governing equations for a rotating fluid layer with an internal heat generation are:

$$\nabla \cdot V = 0, \tag{3}$$

$$\rho_0\left[\frac{\partial V}{\partial t} + (V \cdot \nabla)V + 2\Omega \times V\right] = -\nabla p - \rho g \mathbf{e}_z + \mu\nabla^2 V, \tag{4}$$

$$\frac{\partial T}{\partial t} + (V \cdot \nabla)T = \kappa\nabla^2 T + Q, \tag{5}$$

where the fluid velocity $V = (u, v, w)$, T is the temperature, μ is the viscosity, κ is the thermal diffusivity, K is the thermal conductivity, Q is the uniform internal

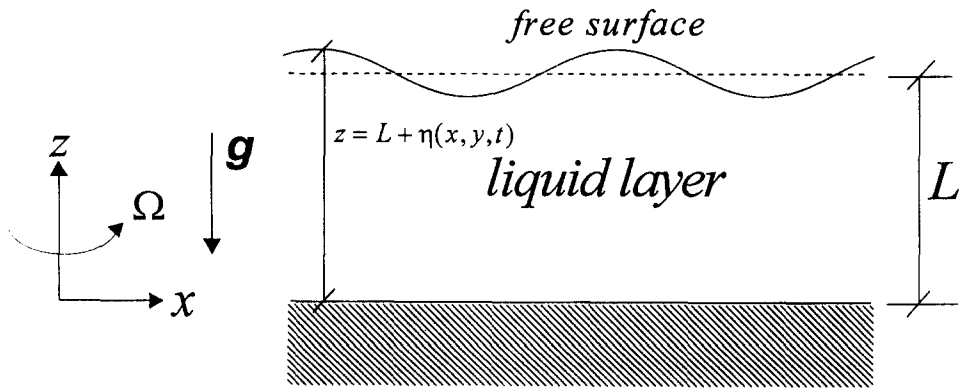

Fig. 1. Physical model.

heat generation, p is the pressure, $\boldsymbol{g}$ is the gravity and $\mathbf{e}_z = [0, 0, 1]$ is a unit vector in the z-direction.

At the deformably free upper surface, at $z = L + \eta(x, y, t)$, the boundary conditions are [8–13]:

$$\frac{\partial \eta}{\partial t} + u\frac{\partial \eta}{\partial x} + v\frac{\partial \eta}{\partial y} = w, \tag{6a}$$

$$K\nabla T \cdot \mathbf{n} + HT = 0, \tag{6b}$$

$$2\mu D_{nt} = \frac{\partial \gamma}{\partial T}\nabla T \cdot \mathbf{t}, \tag{6c}$$

$$(p_a - p) + 2\mu D_{nn} = \gamma \nabla \cdot \mathbf{n}, \tag{6d}$$

where H is the heat transfer coefficient, p_a is the pressure of the atmosphere, D_{ij} is the rate of strain tensor, $\mathbf{t}$ and $\mathbf{n}$ denote tangential and normal unit vectors, respectively, and γ is the surface tension.

For the steady state, the upper free surface is planar and the fluid layer is static and conductive. The pressure and temperature fields are:

$$\bar{p}(z) = p_0 - \rho_0 \boldsymbol{g}(z - L)\left[1 + \frac{\alpha \Delta T}{2L}(z - L)\right], \tag{7a}$$

$$\bar{T}(z) = -\frac{Q}{2\kappa}z^2 + \left(\frac{QL}{2\kappa} - \frac{\Delta T}{L}\right)z + T_0, \tag{7b}$$

where ΔT is the difference of the temperature across the fluid layer and p_0 is the reference pressure.

We may introduce infinitesimal disturbances to the governing equations and boundary conditions by setting

$$(u, v, w, \rho, p, T) = (0, 0, 0, \bar{\rho}, \bar{p}, \bar{T}) + (u', v', w', \rho', p', \theta'), \tag{8}$$

where the primed quantities represent the perturbed variables. Assuming scales L, L^2/κ, κ/L, ΔT and κ/L^2 for coordinates, time, velocity, temperature and vorticity, respectively, then the governing equations of the perturbed state for the liquid layer in the dimensionless forms are:

$$\frac{1}{Pr}\frac{\partial \zeta'}{\partial t} = \nabla^2 \zeta' + \mathscr{J}^{1/2}\frac{\partial w'}{\partial z}, \tag{9}$$

$$\frac{1}{Pr}\frac{\partial}{\partial t}(\nabla^2 w') + \mathscr{J}^{1/2}\frac{\partial \zeta'}{\partial z} = R\nabla_h^2 \theta' + \nabla^4 w', \tag{10}$$

$$\frac{\partial \theta'}{\partial t} + [N_S(1 - 2z) - 1]w' = \nabla^2 \theta', \tag{11}$$

where $\zeta' = \mathbf{e}_z \cdot \nabla \times V'$ is the vorticity in the z-direction, $\nabla^2 = \partial^2/\partial x^2 + \partial^2/\partial y^2 + \partial^2/\partial z^2$ is the Laplacian operator and $\nabla_h^2 = \partial^2/\partial x^2 + \partial^2/\partial y^2$ is the horizontal Laplacian operator. N_S is a dimensionless heat source strength [4] which is defined as:

$$N_S = \frac{QL^2}{2\kappa \Delta T}, \tag{12a}$$

Pr, R and $\mathscr{J}$ are the Prandtl number, Rayleigh number and Taylor number, respectively, and are defined as:

$$Pr = \nu/\kappa, \quad R = \alpha g \Delta T L^3/\nu\kappa, \quad \mathscr{J} = 4\Omega^2 L^4/\nu^2. \tag{12b}$$

Similarly, the perturbed boundary conditions in the dimensionless forms at the free upper surface (at $z = 1$) are:

$$\frac{\partial Z'}{\partial t} = w', \tag{13a}$$

$$\frac{\partial \theta'}{\partial z} - Bi(N_S + 1)Z' + Bi\,\theta' = 0, \tag{13b}$$

$$\left(\frac{\partial^2}{\partial z^2} - \nabla_h^2\right)w' + M(N_S + 1)\nabla_h^2 Z' - M\nabla_h^2 \theta' = 0, \tag{13c}$$

$$C\left[\frac{-1}{Pr}\frac{\partial}{\partial t} + \left(\frac{\partial^2}{\partial z^2} + 3\nabla_h^2\right)\right]\frac{\partial w'}{\partial z} + (Bo - \nabla_h^2)\nabla_h^2 Z' - C\mathscr{J}^{1/2}\zeta' = 0, \tag{13d}$$

$$\frac{\partial \zeta'}{\partial z} = 0, \tag{13e}$$

where Z' is the dimensionless surface deflection and the Crispation number C, Biot number Bi, Bond num-

ber Bo and Marangoni number M are defined, respectively, as:

$$C = \mu\kappa/\gamma L, \quad Bi = HL/K, \quad Bo = \rho g L^2/\gamma,$$
$$M = \tau \Delta T L/\mu\kappa. \tag{14}$$

The perturbed boundary conditions in the dimensionless forms at the lower rigid surface (at $z = 0$) are:

$$w' = \frac{\partial w'}{\partial z} = \zeta' = \theta' = 0. \tag{15}$$

The perturbation quantities in a normal mode form are:

$$\begin{bmatrix} w' \\ \theta' \\ \zeta' \\ Z' \end{bmatrix} = \begin{bmatrix} W(z) \\ \Theta(z) \\ \zeta(z) \\ Z \end{bmatrix} \exp\left[i(a_x x + a_y y) + \sigma t\right], \tag{16}$$

where a_x and a_y are the wavenumbers of the disturbances in the x and y directions, respectively, and σ is the growth parameter, which is a complex variable in general. We denote $\sigma = \sigma_r + i\sigma_i$, where σ_r is the growth rate of the instability and σ_i is the frequency. If $\sigma_r > 0$, the disturbances grow and the system becomes unstable. If $\sigma_r < 0$, the disturbances decay and the system becomes stable. When $\sigma_r = 0$, the instability of the system, at the marginal state, sets in stationarily, provided ($\sigma_i = 0$), or oscillatorily, provided ($\sigma_i \neq 0$).

By substituting equation (16) into equations (9)–(11), we have, setting $\sigma_r = 0$,

$$\left[\frac{i\sigma_i}{Pr} - (D^2 - a^2)\right]\zeta = \mathscr{J}^{1/2} DW, \tag{17}$$

$$\left[\frac{i\sigma_i}{Pr} - (D^2 - a^2)\right](D^2 - a^2)W + \mathscr{J}^{1/2} D\zeta = -a^2 R\Theta, \tag{18}$$

$$[i\sigma_i - (D^2 - a^2)]\Theta + [N_S(1 - 2z) - 1]W = 0, \tag{19}$$

where the operator $D = \partial/\partial z$ and $a = \sqrt{a_x^2 + a_y^2}$ is the wavenumber of the disturbances.

The boundary conditions at the free upper surface (at $z = 1$) are:

$$W = i\sigma_i Z, \tag{20a}$$
$$(D + Bi)\Theta = Bi(N_S + 1)Z, \tag{20b}$$
$$(D^2 + a^2)W + Ma^2\Theta - Ma^2 Z(N_S + 1) = 0, \tag{20c}$$
$$C\left[\frac{i\sigma_i}{Pr} - (D^2 - 3a^2)\right]DW + Bo\, a^2 Z + a^4 Z + C\mathscr{J}^{1/2}\zeta = 0, \tag{20d}$$
$$D\zeta = 0, \tag{20e}$$

and the boundary conditions at the lower surface (at $z = 0$) are:

$$W = DW = \Theta = \zeta = 0. \tag{21}$$

NUMERICAL PROCEDURE

The governing equations (17)–(19) and boundary conditions (20) and (21) form a Sturm–Liouville's problem with the Rayleigh number R or Marangoni number M being the eigenvalue and other physical parameters such as: Pr, $\mathscr{J}$, N_S, C, Bo, Bi and a being fixed. The Runge–Kutta–Gill's shooting method [23, 24] is used to solve the problem. The first step in the procedure is to write equations (17)–(19) as a system of first-order equations,

$$W = u_1, \tag{22}$$
$$DW = Du_1 = u_2, \tag{23a}$$
$$D^2 W = Du_2 = u_3, \tag{23b}$$
$$D^3 W = Du_3 = u_4, \tag{23c}$$
$$\Theta = u_5,$$
$$D\Theta = Du_5 = u_6, \tag{23d}$$
$$\zeta = u_7,$$
$$D\zeta = Du_7 = u_8, \tag{23e}$$

and we obtain

$$D^2\zeta = Du_8 = \left(\frac{i\sigma_i}{Pr} + a^2\right)u_7 - \mathscr{J}^{1/2}u_2, \tag{23f}$$

$$D^2\Theta = Du_6 = (i\sigma_i + a^2)u_5 + [N_S(1 - 2z) - 1]u_1, \tag{23g}$$

$$D^4 W = Du_4 = \left(\frac{i\sigma_i}{Pr} + 2a^2\right)u_3 - \left(\frac{i\sigma_i}{Pr} + a^2\right)a^2 u_1 + a^2 R u_5 + \mathscr{J}^{1/2}u_8. \tag{23h}$$

The shooting procedure starts from the upper boundary, at $z = 1$, and tries to match the boundary conditions at the lower boundary, at $z = 0$. The upper boundary conditions (20a)–(20e) at $z = 1$ can be expressed as:

$$u_1 = \left[-\frac{3i\sigma_i C}{Bo + a^2} + \frac{\sigma_i^2 C}{(Bo + a^2)a^2 Pr}\right]u_2 + \frac{i\sigma_i C}{(Bo + a^2)a^2}u_4 - \frac{i\sigma_i C\mathscr{J}^{1/2}}{(Bo + a^2)a^2}u_7, \tag{24a}$$

$$u_3 = \left[\frac{3i\sigma_i C a^2}{Bo + a^2} - \frac{\sigma_i^2 C}{(Bo + a^2)Pr} - \frac{3MC(N_S + 1)a^2}{Bo + a^2} - \frac{i\sigma_i MC(N_S + 1)}{(Bo + a^2)Pr}\right]u_2 + \left[-\frac{i\sigma_i C}{Bo + a^2} + \frac{MC(N_S + 1)}{Bo + a^2}\right]u_4$$

$$-Ma^2u_5+\left[-\frac{MC\mathscr{J}^{1/2}(N_S+1)}{Bo+a^2}+\frac{i\sigma_i C\mathscr{J}^{1/2}}{Bo+a^2}\right]u_7, \tag{24b}$$

$$u_6=\left[-\frac{i\sigma_i Bi\,C(N_S+1)}{(Bo+a^2)a^2Pr}-\frac{3Bi\,C(N_S+1)}{Bo+a^2}\right]u_2+\frac{Bi\,C(N_S+1)}{(Bo+a^2)a^2}u_4-Bi\,u_5-\frac{Bi\,C\mathscr{J}^{1/2}(N_S+1)}{(Bo+a^2)a^2}u_7, \tag{24c}$$

$$u_8=0. \tag{24d}$$

We shall guess four boundary conditions,

$$u_2=c_1,\quad u_4=c_2,\quad u_5=c_3\quad\text{and}\quad u_7=c_4,$$

then the general form of the solution becomes:

$$U=c_1U_1+c_2U_2+c_3U_3+c_4U_4, \tag{25}$$

where

$$U=[u_1,u_2,u_3,u_4,u_5,u_6,u_7,u_8]^T, \tag{26a}$$

$$U_1=\left[-\frac{3i\sigma_iC}{Bo+a^2}+\frac{\sigma_i^2C}{(Bo+a^2)a^2Pr},1,\frac{3i\sigma_iCa^2}{Bo+a^2}-\frac{\sigma_i^2C}{(Bo+a^2)Pr}-\frac{3MC(N_S+1)a^2}{Bo+a^2}-\frac{i\sigma_iMC(N_S+1)}{(Bo+a^2)Pr},0,0,-\frac{3Bi\,C(N_S+1)}{Bo+a^2}-\frac{i\sigma_iBi\,C(N_S+1)}{(Bo+a^2)a^2Pr},0,0\right]^T, \tag{26b}$$

$$U_2=\left[\frac{i\sigma_iC}{(Bo+a^2)a^2},0,-\frac{i\sigma_iC}{Bo+a^2}+\frac{MC(N_S+1)}{Bo+a^2},1,0,\frac{Bi\,C(N_S+1)}{(Bo+a^2)a^2},0,0\right]^T, \tag{26c}$$

$$U_3=[0,0,-Ma^2,0,1,-Bi,0,0]^T, \tag{26d}$$

$$U_4=\left[-\frac{i\sigma_iC\mathscr{J}^{1/2}}{(Bo+a^2)a^2},0,-\frac{MC\mathscr{J}^{1/2}(N_S+1)}{(Bo+a^2)}+\frac{i\sigma_iC\mathscr{J}^{1/2}}{(Bo+a^2)},0,0,-\frac{Bi\,C\mathscr{J}^{1/2}(N_S+1)}{(Bo+a^2)a^2},1,0\right]^T. \tag{26e}$$

We may guess a value for M and assume each of U_i, $i=1, 2, 3, 4$, in (26b)–(26e) as a set of initial conditions. Then we start shooting from $z=1$ and try to match the boundary conditions at $z=0$. The results finally turn into a matrix form,

$$\begin{bmatrix}U_1^1 & U_2^1 & U_3^1 & U_4^1\\ U_1^2 & U_2^2 & U_3^2 & U_4^2\\ U_1^5 & U_2^5 & U_3^5 & U_4^5\\ U_1^7 & U_2^7 & U_3^7 & U_4^7\end{bmatrix}\begin{bmatrix}c_1\\c_2\\c_3\\c_4\end{bmatrix}=0, \tag{27}$$

where U_i^k is the kth element of U_i. The determinant of equation (27) is complex, but its real and imaginary parts should vanish separately for c_i being nontrivial. The eigenvalue problem is thus established as:

$$f(i\sigma_i, R, M, Pr, \mathscr{J}, N_S, C, Bo, Bi, a)=0, \tag{28}$$

where f is the determinant of the complex matrix and is equal to $\mathrm{Re}(f)+i\,\mathrm{Im}(f)$. Equation (28) is solved directly, using the Broyden's method [24], and the eigenvalue R or M and the frequency σ_i is thus obtained.

For each step, approximations $\mathbf{x}^{(n-1)}=[M,\sigma_i]^T$ and the Jacobian matrix $\mathbf{J}(\mathbf{x}^{(n-1)})$, being $[A^{(n-1)}]^{-1}$, are needed. Then we will have a correcting matrix as follows

$$[A^{(n)}]^{-1}=[A^{(n-1)}]^{-1}+\frac{\{\mathbf{s}^{(n)}-[A^{(n-1)}]^{-1}\mathbf{y}^n\}[\mathbf{s}^{(n)}]^T[A^{(n-1)}]^{-1}}{[\mathbf{s}^{(n)}]^T[A^{(n-1)}]^{-1}\mathbf{y}^n}, \tag{29}$$

where the notation $\mathbf{y}^n=f(\mathbf{x}^{(n)})-f(\mathbf{x}^{(n-1)})$ and $\mathbf{s}^{(n)}=\mathbf{x}^{(n)}-\mathbf{x}^{(n-1)}$. The next approximation will be

$$\mathbf{x}^{(n+1)}=\mathbf{x}^{(n)}-[A^{(n)}]^{-1}f(\mathbf{x}^{(n)}). \tag{30}$$

The iteration is terminated when the approximate value of determinant f is less than 10^{-6}. For fixed parameters, Marangoni number M or Rayleigh number R and frequency σ_i are obtained for various wavenumbers a. The critical value M_c or R_c, having a minimum value on the surface in $(a, M, i\sigma_i)$ or $(a, R, i\sigma_i)$ space, marks the onset of the Bénard–Marangoni convection, stationary or oscillatory, at the marginal state.

RESULTS AND DISCUSSION

For Marangoni instability (i.e. $R=0$) with $C=10^{-6}$–10^{-1}, the critical conditions $[M_c, a_c, \sigma_{ic}]$ compare very well with the results of Pérez-García and Carneiro [13] and are listed in Table 1. The parameter values chosen are $Pr=1$, $B_o=0.1$ and $B_i=0$. For the Marangoni number M being negative, the surface tension increases with the increasing temperature and oscillatory modes become possible, as predicted previously [11–15]. Oscillatory modes cease to appear for $M>0$, in which range the surface tension decreases with increasing temperature. The critical Marangoni number, being negative, in the absolute form $|M_c|$ and its associated frequency σ_{ic} as functions of the Crispation number C for selected values of the Prandtl number Pr are plotted in Figs. 2(a) and (b). The absolute values of critical Marangoni number $|M_c|$ decrease with the Crispation number C and increase

Table 1. Numerically calculated values of M_c, a_c and σ_{ic} for different values of C on the oscillatory instability of Marangoni convection without the thermal buoyancy ($Bo = 0.1$, $Bi = 0$ and $\mathcal{J} = N_S = R = 0$)

	Data from ref. [13] $Pr = 1.0$			Present study $Pr = 1.0$			$Pr = 0.1$		
C	M_c	a_c	σ_{ic}	M_c	a_c	σ_{ic}	M_c	a_c	σ_{ic}
0	—	—	—	—	—	—	—	—	—
10^{-6}	−62 785.97	0.08	26	−62 785.117	0.080	26.106	−27 339.290	0.073	7.551
10^{-5}	−8554.13	0.18	21	−8552.231	0.178	20.775	−3331.287	0.131	4.561
10^{-4}	−1896.11	0.34	17	−1895.632	0.346	16.551	−545.415	0.232	3.010
10^{-3}	−1075.92	0.59	17	−1075.895	0.591	16.610	−144.761	0.391	2.216
10^{-2}	−1044.56	0.28	6.7	−1043.880	0.283	6.753	−70.086	0.517	1.572
10^{-1}	−1016.23	0.28	6.7	−1015.898	0.282	6.584	−65.541	0.538	1.316

with the Prandtl number Pr. The Crispation number C, associated with the inverse effect of the surface tension, does show the rigidity of the deformably free upper surface. For the Crispation number C to be zero, the upper surface, subject to an infinite surface tension, is taken to be undeformably flat and the system becomes more stabilizing for Marangoni convective instabilities. Therefore, the existence of stationary modes is expected. For larger values of Crispation number C, the oscillatory modes may exist, corresponding to lower absolute values of the critical Marangoni number $|M_c|$. The deformability degree of the free upper surface illustrates a destabilizing effect. The absolute values of critical Marangoni number $|M_c|$ increase with the Prandtl number Pr, because of the increasing viscosity of the fluid layer. Also the corresponding frequency σ_{ic} has the increasing trends.

In Table 2, the critical conditions $[M_c, a_c, \sigma_{ic}]$ for $Bi = 0, 0.05$ and $\mathcal{J} = 0$, $C = 10^{-5}$ and $Pr = 0.02$ compare very well with those of Wilson [15], provided magnetic effects are absent. Also tabulated in Table 2 are cases for various values of Bi and $\mathcal{J}$. Figures 3(a) and (b) show the absolute values of critical Marangoni number $|M_c|$ and frequency σ_{ic} as functions of Taylor number $\mathcal{J}$ for selected values of Biot number $Bi = 0$, 0.05 and 0.1. The critical conditions $[|M_c|, \sigma_{ic}]$ increase monotonically with the Taylor number $\mathcal{J}$, as the Taylor–Proudman theorem [2] predicts that all steady slow motion of inviscid flow in a rotating system are necessarily two-dimensional. The effect of rotation suppresses the onset of convection and raises the stability of the system.

Physically, the more the thermal energy is conducted away, the less it is stored in the liquid layer so that the system tends to be more stable. The influence of the heat transfer at the free upper surface to the system is shown in Figs. 4(a) and (b) and is tabulated in Table 2. When the upper surface is perfectly insulated, $B_i = 0$, the dissipation of thermal disturbances into the ambient surrounding is extremely poor and the system becomes more destabilizing. When the upper surface is perfectly conducting, $Bi \to \infty$, this dissipation is effective and the system becomes less destabilizing. The critical conditions $[|M_c|, \sigma_{ic}]$ increase with the Biot number Bi.

The effect of a non-linear temperature distribution, induced by an internal heat generation, is considered. Figures 5(a) and (b) and Table 3 show the critical

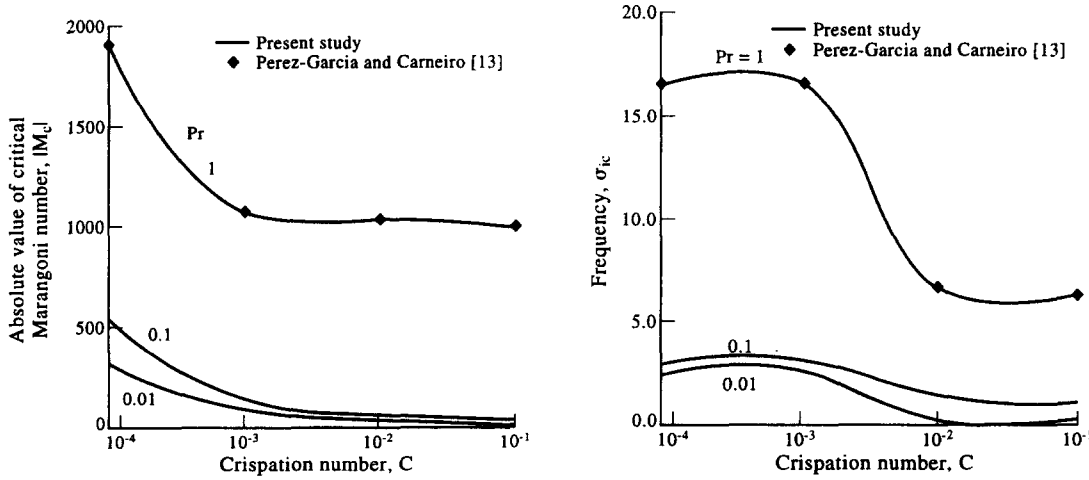

Fig. 2. (a) The absolute value of critical Marangoni number $|M_c|$ plotted as functions of C for $Pr = 1$, 0.1, 0.01 on the oscillatory instability of Marangoni convection in the case $Bo = 0.1$, $Bi = 0$ and $\mathcal{J} = N_S = R = 0$. (b) The critical frequency σ_{ic} plotted as functions of C for $Pr = 1$, 0.1, 0.01 on the oscillatory instability of Marangoni convection in the case $Bo = 0.1$, $Bi = 0$ and $\mathcal{J} = N_S = R = 0$.

Table 2. Numerically calculated values of M_c, a_c and σ_{ic} for different values of $\mathscr{J}$ and Bi on the oscillatory instability of the Bénard–Marangoni convection ($C = 10^{-5}$, $Pr = 0.02$, $Bo = 0.01$ and $R = N_S = 0$)

	$Bi = 0$			$Bi = 0.05$			$Bi = 0.1$		
$\mathscr{J}$	M_c	a_c	σ_{ic}	M_c	a_c	σ_{ic}	M_c	a_c	σ_{ic}
0	−952.403	0.2015	2.0863	−1027.587	0.2071	2.1914	−1105.408	0.2126	2.2972
	(−952.41	0.2015	2.0864)†	(−1027.60	0.2071	2.1916)			
1	−952.448	0.2015	2.0864	−1027.631	0.2071	2.1915	−1105.453	0.2126	2.2973
10	−952.853	0.2016	2.0890	−1028.034	0.2072	2.1941	−1105.852	0.2126	2.2981
100	−956.868	0.2020	2.1044	−1032.029	0.2076	2.2092	−1109.818	0.2131	2.3149
1000	−994.175	0.2057	2.2490	−1069.287	0.2115	2.3556	−1146.931	0.2171	2.4617
2000	−1031.131	0.2086	2.3826	−1106.380	0.2147	2.4924	−1184.058	0.2205	2.6003
2500	−1048.311	0.2096	2.4399	−1123.672	0.2160	2.5536	−1201.413	0.2218	2.6608
5000	−1125.246	0.2130	2.6860	−1201.423	0.2204	2.8105	−1279.718	0.2269	2.9254
7500	−1191.936	0.2139	2.8763	−1269.173	0.2227	3.0161	−1348.232	0.2302	3.1429
10000	−1251.754	0.2133	3.0340	−1330.188	0.2238	3.1914	−1410.119	0.2323	3.3289

	$Bi = 0.25$			$Bi = 0.5$			$Bi = 0.75$		
$\mathscr{J}$	M_c	a_c	σ_{ic}	M_c	a_c	σ_{ic}	M_c	a_c	σ_{ic}
0	−1355.080	0.2283	2.6143	−1827.177	0.2535	3.1677	−2372.189	0.2783	3.7648
1	−1355.123	0.2283	2.6144	−1827.217	0.2535	3.1677	−2372.226	0.2783	3.7649
10	−1355.509	0.2284	2.6170	−1827.574	0.2535	3.1683	−2372.557	0.2783	3.7654
100	−1395.346	0.2288	2.6316	−1831.136	0.2539	3.1826	−2375.852	0.2786	3.7772
1000	−1395.615	0.2328	2.7753	−1865.326	0.2573	3.3109	−2407.846	0.2813	3.8876
2000	−1432.416	0.2363	2.9124	−1900.783	0.2605	3.4384	−2441.596	0.2840	4.0015
2500	−1449.753	0.2378	2.9748	−1917.692	0.2619	3.4970	−2457.856	0.2852	4.0543
5000	−1528.723	0.2438	3.2471	−1995.901	0.2678	3.7587	−2534.098	0.2905	4.2968
7500	−1598.520	0.2482	3.4756	−2066.136	0.2725	3.9851	−2603.612	0.2950	4.5135
10000	−1661.951	0.2517	3.6771	−2130.543	0.2764	4.1869	−2667.941	0.2988	4.7081

†The values in parentheses are obtained from Wilson [15].

conditions $[|M_c|, \sigma_{ic}]$ in terms of the Bond number Bo for selected values of the dimensionless heat source strength N_S. The case $N_S = 0$ represents a linear temperature distribution. As N_S increases positively, the non-linear temperature distribution of the parabolic type does enhance thermal disturbances in the upper part of the fluid layer and a more destabilizing state than a linear one for the Marangoni instability is thus established. The absolute value of critical Marangoni number $|M_c|$, from Fig. 5(a), decreases with N_S quite rapidly for small values of N_S and rather slowly for large values of N_S. However, Fig. 5(b) shows that, with the dimensionless heat source strength N_S, the frequency σ_{ic} increases for $Bo \geqslant 0.1$ and decreases for $Bo < 0.1$. Figures 5(a) and (b) also show that the absolute value of critical Marangoni number $|M_c|$ and frequency σ_{ic} increase with the Bond number Bo, mainly due to the property of the stabilizing effect

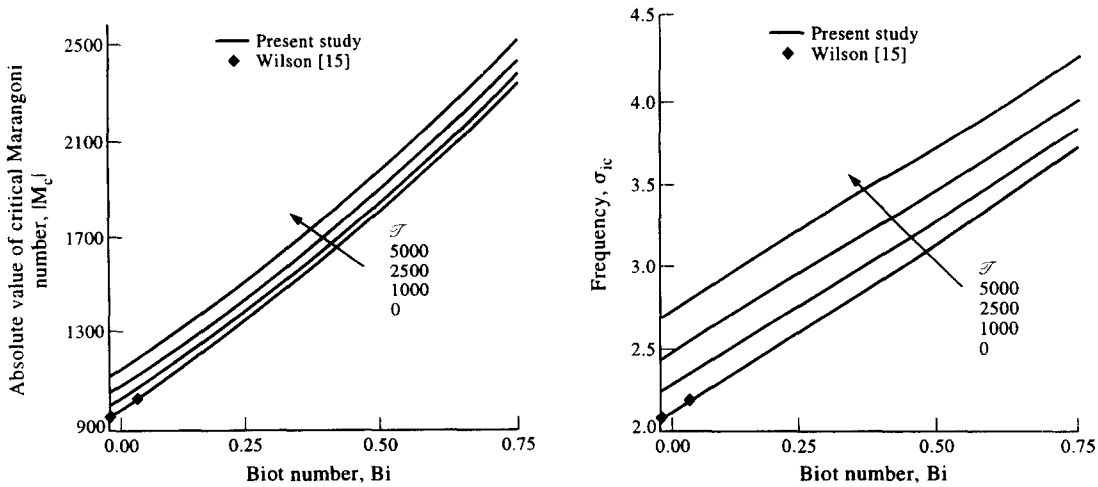

Fig. 3. (a) The absolute value of critical Marangoni number $|M_c|$ plotted as functions of Bi for $\mathscr{J} = 0$, 1000, 2500, 5000 on the oscillatory instability of Bénard–Marangoni convection in the case $C = 10^{-5}$, $Pr = 0.02$, $Bo = 0.01$ and $N_S = R = 0$. (b) The critical frequency σ_{ic} plotted as functions of Bi for $\mathscr{J} = 0$, 1000, 2500, 5000 on the oscillatory instability of Bénard–Marangoni convection in the case $C = 10^{-5}$, $Pr = 0.02$, $Bo = 0.01$ and $N_S = R = 0$.

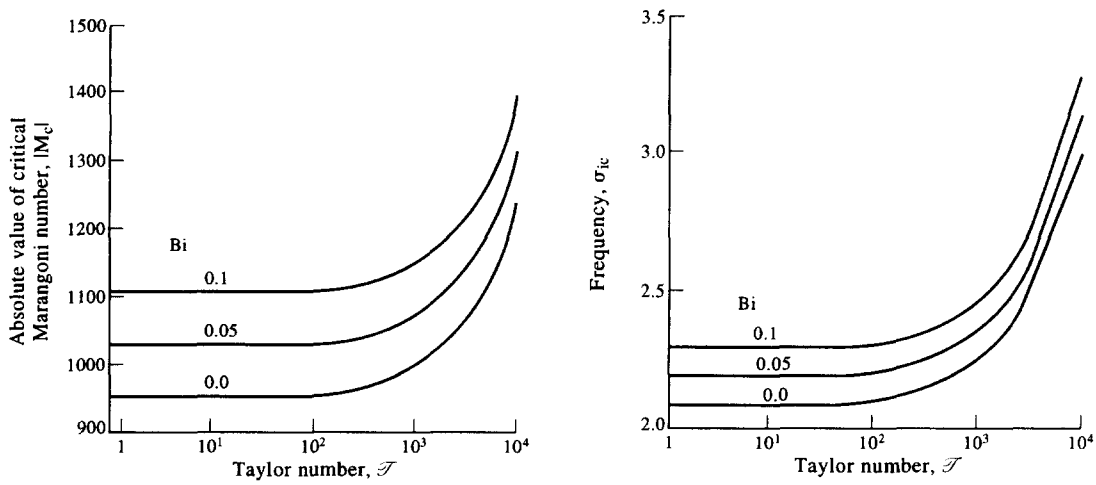

Fig. 4. (a) The absolute value of critical Marangoni number $|M_c|$ plotted as functions of $\mathscr{J}$ for $Bi = 0$, 0.05, 0.1 on the oscillatory instability of Bénard–Marangoni convection in the case $C = 10^{-5}$, $Pr = 0.02$, $Bo = 0.01$ and $N_S = R = 0$. (b) The critical frequency σ_{ic} plotted as functions of $\mathscr{J}$ for $Bi = 0$, 0.05, 0.1 on the oscillatory instability of Bénard–Marangoni convection in the case $C = 10^{-5}$, $Pr = 0.02$, $Bo = 0.01$ and $N_S = R = 0$.

of gravitation on the free upper surface. The Bond number Bo, measuring the relative effect of gravity on the surface tension, indicates the dominant one of flattening a curved free upper surface. With the Crispation number fixed, the gravity force acts as the sole and stabilizing effect. The increasing trend of $|M_c|$ with Bond number Bo becomes significant for $N_S < 1$ and also for $N_S > 1$ in the range $0 < Bo < 0.01$ and moderately for $N_S > 1$ in the range $Bo > 0.01$. The frequency σ_{ic} increases monotonically with the Bond number Bo, except a rapid increase occurs for $N_S > 1$ in the range $0 < Bo < 0.01$.

The absolute value of the critical Marangoni number $|M_c|$ and the frequency σ_{ic} versus the Rayleigh number R for various values of $\mathscr{J}$ are plotted in Figs. 6(a) and (b) and are listed in Table 4. The range of the Rayleigh number R is chosen from 0 to 669. If a linear temperature profile is imposed across the fluid layer, pure thermal convection becomes possible, provided the Rayleigh number R reaches a critical value 669 [2–5]. While considering Rayleigh–Marangoni convective instability, the effects of the thermal buoyancy and surface tension interact mutually and reinforce each other. From Fig. 6(a), the stability curves in the (M_c, R) plane show a linear relation. The absolute value of the critical Marangoni number $|M_c|$ decreases linearly with the Rayleigh number R, irrespective of the Taylor number $\mathscr{J}$. However, from Fig. 6(b), with Rayleigh number R, the frequency σ_{ic} decreases slightly for $\mathscr{J} \leqslant 10^3$ and increases slightly for $\mathscr{J} > 10^3$.

Figures 7(a) and (b) show the effect of the Taylor

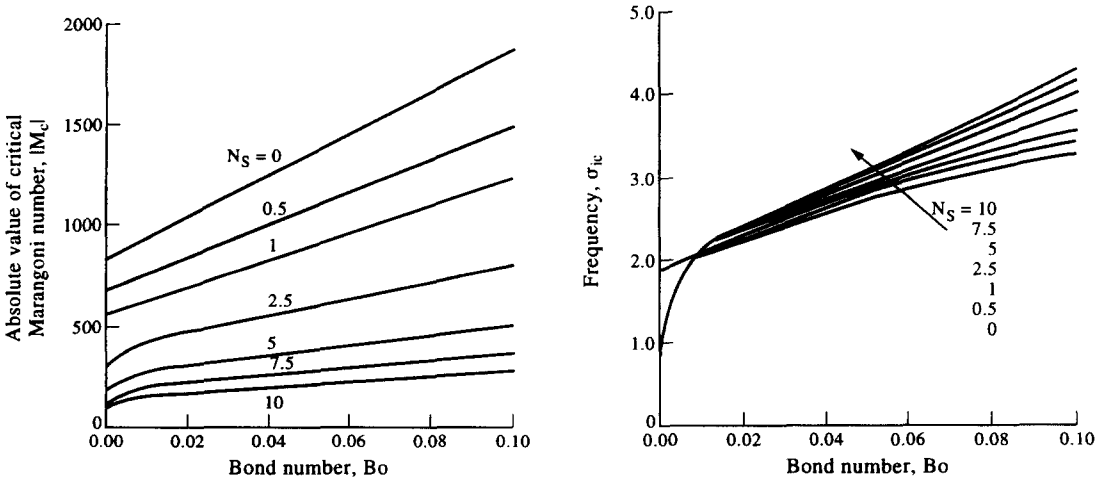

Fig. 5. (a) The absolute value of critical Marangoni number $|M_c|$ plotted as functions of Bo for $N_S = 0$–10 on the oscillatory instability of Bénard–Marangoni convection in the case $C = 10^{-5}$, $Pr = 0.02$, $Bi = 0$ and $\mathscr{J} = R = 0$. (b) The critical frequency σ_{ic} plotted as functions of Bo for $N_S = 0$–10 on the oscillatory instability of Bénard–Marangoni convection in the case $C = 10^{-5}$, $Pr = 0.02$, $Bi = 0$ and $\mathscr{J} = R = 0$.

Table 3. Numerically calculated values of M_c, a_c and σ_{ic} for different values of Bo and N_S on the oscillatory instability of the Bénard–Marangoni convection ($C = 10^{-5}$, $Pr = 0.02$, $Bi = 0$ and $\mathcal{J} = R = 0$)

	$Bo = 0$			$Bo = 0.01$			$Bo = 0.025$		
N_S	M_c	a_c	σ_{ic}	M_c	a_c	σ_{ic}	M_c	a_c	σ_{ic}
0.0	−848.979	0.1989	1.8420	−952.403	0.2015	2.0863	−1105.914	0.2024	2.3708
0.5	−682.634	0.1962	1.8330	−766.878	0.2007	2.1098	−890.343	0.2028	2.4167
1.0	−562.192	0.1209	0.8303	−640.904	0.2000	2.1220	−744.122	0.2030	2.4457
2.5	−308.950	0.0872	0.5159	−428.227	0.1982	2.1304	−497.394	0.2033	2.4927
5.0	−185.819	0.0863	0.5140	−275.196	0.1965	2.1284	−319.836	0.2035	2.5252
7.5	−132.830	0.0859	0.5130	−202.630	0.1955	2.1238	−235.591	0.2035	2.5386
10.0	−103.350	0.0857	0.5127	−160.322	0.1948	2.1190	−186.450	0.2036	2.5482
	$Bo = 0.05$			$Bo = 0.075$			$Bo = 0.1$		
N_S	M_c	a_c	σ_{ic}	M_c	a_c	σ_{ic}	M_c	a_c	σ_{ic}
0.0	−1362.993	0.2016	2.7463	−1623.347	0.2000	3.0556	−1887.111	0.1982	3.3236
0.5	−1095.150	0.2035	2.8233	−1300.822	0.2033	3.1648	−1507.671	0.2030	3.4696
1.0	−914.046	0.2049	2.8772	−1083.517	0.2059	3.2460	−1252.882	0.2070	3.5851
2.5	−609.511	0.2075	2.9719	−719.722	0.2112	3.4022	−828.263	0.2157	3.8247
5.0	−391.205	0.2098	3.0482	−460.418	0.2161	3.5384	−527.514	0.2246	4.0599
7.5	−287.894	0.2110	3.0864	−338.227	0.2189	3.6137	−386.526	0.2303	4.2075
10.0	−227.714	0.2118	3.1108	−267.228	0.2207	3.6614	−304.874	0.2343	4.3105

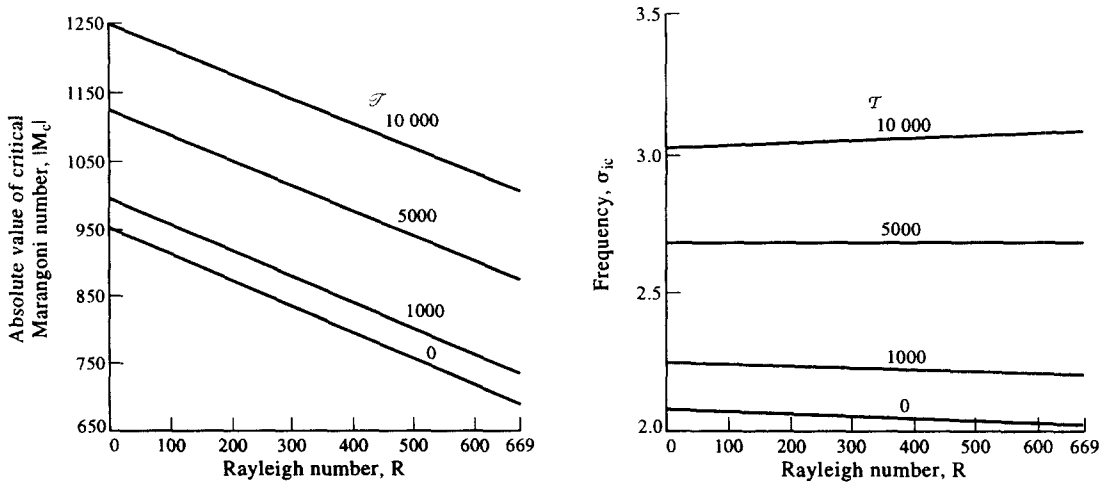

Fig. 6. (a) The absolute value of critical Marangoni number $|M_c|$ plotted as functions of R for $\mathcal{J} = 0$, 1000, 5000, 10 000 on the oscillatory instability of Bénard–Marangoni convection in the case $C = 10^{-5}$, $Pr = 0.02$, $Bo = 0.01$, $Bi = 0$ and $N_S = 0$. (b) The critical frequency σ_{ic} plotted as functions of R for $\mathcal{J} = 0$, 1000, 5000, 10 000 on the oscillatory instability of Bénard–Marangoni convection in the case $C = 10^{-5}$, $Pr = 0.02$, $Bo = 0.01$, $Bi = 0$ and $N_S = 0$.

number $\mathcal{J}$ on the absolute value of the critical Marangoni number $|M_c|$ and the frequency σ_{ic} for various values of the Rayleigh number R. The dashed curves correspond to the limiting case (i.e. $R = 669$), at which stationary thermal convection may take place in the fluid layer and below which the Marangoni instability would become dominant. As expected, $|M_c|$ and σ_{ic} increase with the Taylor number $\mathcal{J}$ slightly for $\mathcal{J} < 10^3$ and rapidly for $\mathcal{J} > 10^3$. Also shown in Figs. 7(a) and (b), all these curves become coinciding for $\mathcal{J} > 10^4$. Obviously, contrary to that of the thermal buoyancy, the effect of rotation does suppress the system. Significant illustrations of the rotation are depicted in Figs. 3 and 6 as well.

CONCLUSIONS

The effects of rotation and internal heat generation on the onset of oscillatory modes of Bénard–Marangoni instability are analyzed. The following results have been obtained:

(1) Deformation of the upper surface, associated with the Crispation number C, plays a significant role on the onset of oscillatory modes of the Bénard–Marangoni convective instability. The absolute value of the critical Marangoni number $|M_c|$ and its frequency σ_{ic} decrease with the Crispation number C and increase with the Bond number Bo.

(2) Obviously, contrary to that of thermal buoy-

Table 4. Numerically calculated values of M_c, a_c and σ_{ic} for different values of R and $\mathcal{J}$ on the oscillatory instability of the Bénard–Marangoni convection ($C = 10^{-5}$, $Pr = 0.02$, $Bo = 0.01$, $Bi = 0$ and $N_S = 0$)

	$\mathcal{J} = 0$			$\mathcal{J} = 10$			$\mathcal{J} = 100$		
R	M_c	a_c	σ_{ic}	M_c	a_c	σ_{ic}	M_c	a_c	σ_{ic}
0	−952.403	0.2015	2.0863	−952.853	0.2016	2.0890	−956.868	0.2020	2.1044
100	−914.442	0.2016	2.0809	−914.895	0.2016	2.0818	−918.940	0.2021	2.0990
200	−876.464	0.2016	2.0737	−876.921	0.2017	2.0764	−880.997	0.2022	2.0935
300	−838.471	0.2017	2.0682	−838.932	0.2017	2.0692	−843.039	0.2022	2.0864
400	−800.463	0.2017	2.0610	−800.927	0.2018	2.0637	−805.066	0.2023	2.0809
500	−762.438	0.2018	2.0554	−762.906	0.2018	2.0564	−767.078	0.2023	2.0736
600	−724.397	0.2018	2.0482	−724.869	0.2019	2.0508	−729.074	0.2024	2.0681
669	−698.140	0.2019	2.0448	−698.614	0.2019	2.0458	−702.843	0.2024	2.0631
	$\mathcal{J} = 1000$			$\mathcal{J} = 5000$			$\mathcal{J} = 10\,000$		
R	M_c	a_c	σ_{ic}	M_c	a_c	σ_{ic}	M_c	a_c	σ_{ic}
0	−994.175	0.2057	2.2490	−1125.246	0.2130	2.6860	−1251.754	0.2133	3.0340
100	−956.511	0.2059	2.2455	−1088.436	0.2135	2.6877	−1215.873	0.2147	3.0481
200	−918.837	0.2060	2.2403	−1051.619	0.2140	2.6894	−1179.956	0.2160	3.0610
300	−881.153	0.2062	2.2368	−1014.795	0.2144	2.6895	−1144.010	0.2171	3.0711
400	−843.458	0.2063	2.2315	−977.965	0.2149	2.6911	−1108.040	0.2182	3.0813
500	−805.752	0.2065	2.2279	−941.129	0.2154	2.6928	−1072.048	0.2191	3.0886
600	−768.036	0.2066	2.2226	−904.287	0.2158	2.6928	−1036.038	0.2200	3.0960
669	−742.006	0.2067	2.2194	−878.863	0.2161	2.6932	−1011.183	0.2206	3.1008

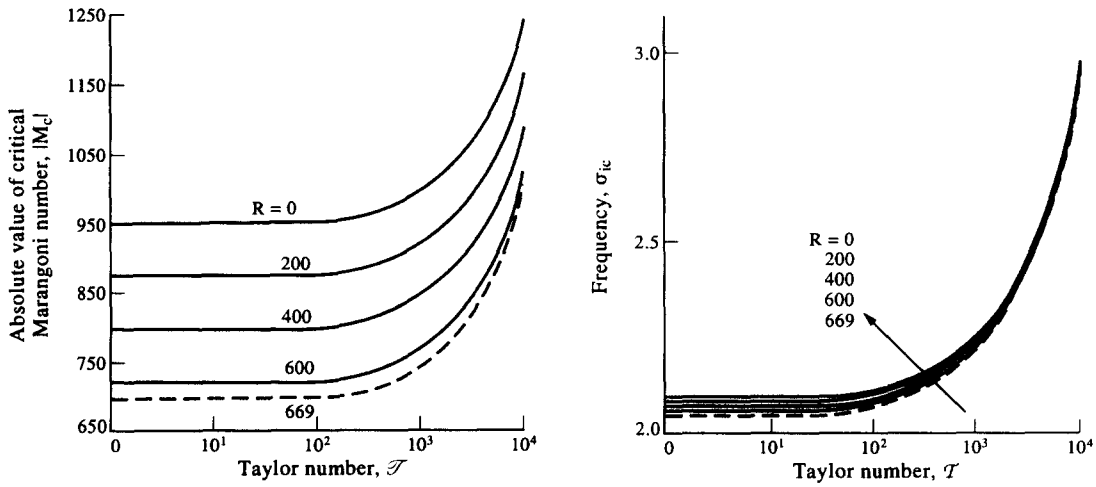

Fig. 7. (a) The absolute value of critical Marangoni number $|M_c|$ plotted as functions of $\mathcal{J}$ for $R = 0$, 200, 400, 600, 669 on the oscillatory instability of Bénard–Marangoni convection in the case $C = 10^{-5}$, $Pr = 0.02$, $Bo = 0.01$, $Bi = 0$ and $N_S = 0$. (b) The critical frequency σ_{ic} plotted as functions of $\mathcal{J}$ for $R = 0$, 200, 400, 600, 669 on the oscillatory instability of Bénard–Marangoni convection in the case $C = 10^{-5}$, $Pr = 0.02$, $Bo = 0.01$, $Bi = 0$ and $N_S = 0$.

ancy, the effect of rotation does suppress the system. Thermal disturbances, originating from the internal heat generation (i.e. N_S), destabilize the system strongly.

(3) The larger the Biot number Bi, the more stable the whole system, as a result of the tendency toward an isothermal state, while a larger Prandtl number Pr does lower the degree of stability.

Acknowledgement—The authors are indebted to the referees for their valuable comments which led to an improvement in the paper.

REFERENCES

1. D. A. Nield, Surface tension and buoyancy effects in cellular convection, *J. Fluid Mech.* **19**, 341–352 (1964).
2. S. Chandrasekhar, *Hydrodynamic and Hydromagnetic Stability*. Oxford University Press, Oxford (1961).
3. P. G. Drazin and W. H. Reid, *Hydrodynamic Stability*. Oxford University Press, Oxford (1961).
4. E. M. Sparrow, R. J. Goldstein and V. K. Jonsson, Thermal instability in a horizontal fluid layer: effect of boundary conditions and non-linear temperature, *J. Fluid Mech.* **18**, 513–529 (1964).
5. E. N. Ferm and D. J. Wollkind, Onset of Rayleigh–Bénard–Marangoni instability: comparison between

theory and experiments, *J. Non-Equilib. Thermodyn.* **9,** 169–170 (1982).
6. J. R. A. Pearson, On convection cell induced by surface tension, *J. Fluid Mech.* **4,** 489–500 (1958).
7. A. Vidal and A. Acrivos, Nature of the neutral state in surface-tension driven convection, *Phys. Fluids* **9,** 615–616 (1966).
8. L. E. Scriven and C. V. Sternling, On cellular convection driven by surface tension gradients: effect of mean surface tension and surface viscosity, *J. Fluid Mech.* **19,** 321–340 (1965).
9. K. A. Smith, On convective instability induced by surface-tension gradients, *J. Fluid Mech.* **24,** 401–414 (1966).
10. S. H. Davis and G. M. Homsy, Energy stability theory for free-surface problem: buoyancy-thermocapillary layers, *J. Fluid Mech.* **98,** 527–553 (1980).
11. R. D. Benguria and M. C. Depassier, Oscillatory instabilities in the Rayleigh–Bénard problem with a free surface, *Phys. Fluids* **30,** 1678–1682 (1987).
12. R. D. Benguria and M. C. Depassier, On the linear stability theory of Bénard–Marangoni convection, *Phys. Fluids* **1,** 1123–1127 (1989).
13. R. Pérez-García and G. Carneiro, Linear stability analysis of Bénard–Marangoni convection in fluids with a deformable free surface, *Phys. Fluids A* **3,** 292–298 (1991).
14. S. K. Wilson, The effect of a uniform magnetic field on the onset of steady Bénard–Marangoni convection in a layer of conducting fluid, *J. Engng Math.* **27,** 161–188 (1993).
15. S. K. Wilson, The effect of a uniform magnetic field on oscillatory Marangoni convection, *Microgravity Sci. Technol.* **VII/3,** 228–233 (1994).
16. P. H. Roberts, Convection in horizontal layers with internal heat generation: theory, *J. Fluid Mech.* **30,** 33–49 (1967).
17. P. D. Gasser and M. S. Kazimi, Onset of convection in a porous medium with internal heat generation, *J. Heat Transfer* **98,** 49–54 (1976).
18. M. Kaviany, Thermal convective instabilities in a porous medium, *J. Heat Transfer* **106,** 137–142 (1984).
19. G. Veronis, Motions at subcritical values of the Rayleigh number in a rotating fluid, *J. Fluid Mech.* **24,** 545–554 (1966).
20. R. Friedrich and N. Rudraiah, Marangoni convection in a rotating fluid layer with non-uniform temperature gradient, *Int. J. Heat Mass Transfer* **27,** 443–449 (1984).
21. A. J. Pearlstein, Effect of rotation on the stability of a doubly diffusive fluid layer, *J. Fluid Mech.* **103,** 389–412 (1981).
22. H. F. Goldstein, E. Knobloch, I. Mercader and M. Net, Convection in a rotating cylinder. Part 1. Linear theory for moderate Prandtl numbers, *J. Fluid Mech.* **248,** 583–604 (1993).
23. A. Davey, *Numerical Methods for the Solution of Linear Differential Eigenvalue Problems*, pp. 485–498. University of Newcastle-upon-Tyne Press, Newcastle-upon-Tyne (1976).
24. R. L. Burden and J. D. Fairs, *Numerical Analysis*. Prindle Weber and Schmidt, Boston, MA (1985).